# The blueschist-bearing Qiangtang metamorphic belt (northern Tibet, China) as an in situ suture zone: Evidence from geochemical comparison with the Jinsa suture

Kai-Jun Zhang* Guangzhou Institute of Geochemistry, Key Laboratory of Geology of Marginal Sea, Chinese Academy of Sciences, Wushan, Guangzhou 510640, China, and Department of Earth Sciences, Nanjing University, Nanjing 210093, China
Yu-Xiu Zhang, Bing Li Guangzhou Institute of Geochemistry, Key Laboratory of Geology of Marginal Sea, Chinese Academy of Sciences, Wushan, Guangzhou 510640, China, and Graduate School, Chinese Academy of Science, Beijing 100008, China
Ying-Tang Zhu College of Earth Sciences, Chengdu University of Technology, Chengdu 610059, China
Rong-Zhu Wei Shanxi Geological Survey, Yuci 030600, Shanxi, China

## ABSTRACT

**Metasiliciclastic rocks and metabasalts from the blueschist-bearing Qiangtang metamorphic belt and the Jinsa suture zone were analyzed for major and trace elements in an attempt to evaluate the affinities of these two tectonic entities. Tholeiitic mid-oceanic-ridge basalts (MORBs) from the Jinsa suture can be distinguished from metabasalts of Qiangtang, which have alkalic compositions and exhibit a range of characteristics typical of many within-plate oceanic islands. The Qiangtang metasiliciclastic rocks were derived from a passive continental margin source, whereas those from the Jinsa suture zone were sourced from a continental island arc or an active continental margin source. The geochemical distinction of metasiliciclastic rocks and metabasalts of the Qiangtang metamorphic belt from their counterparts within the Jinsa suture indicates that there is no affinity between these two tectonic entities and that the Qiangtang metamorphic belt could not have been underthrust from the Jinsa suture. It most likely represents an exhumed accretionary complex composed of sediments derived from a passive continental margin and fragments of seamount sequences, and marks an in situ suture zone that separates northern and southern Qiangtang terranes.**

**Keywords:** Tibet, Qiangtang, Jinsa suture zone, mélange, geochemistry, crustal structure, Tethys.

## INTRODUCTION

A >500 km long and up to 100 km wide blueschist-bearing metamorphic belt is a prominent feature within the interior of the Qiangtang block in the northern Tibetan Plateau (Figs. 1A and 1B). Its origin remains the subject of intense debate and has been interpreted as (1) an in situ paleo-Tethyan suture zone (Shuanghu suture, Fig. 1A) that separates northern and southern Qiangtang (e.g., Li et al., 1995; Bao et al., 1999; Zhang, 2001) (Fig. 1C); (2) an early Mesozoic mélange that was underthrust from the Jinsa suture and then exhumed in the interior of the Qiangtang block (Kapp et al., 2000, 2003; Yin and Harrison, 2000) (Fig. 1D); (3) a late Paleozoic rift (Wang et al., 1987; Deng et al., 1996; Xia et al. 2001). The rift model differs from the other two and is not discussed here because the rifting occurred far earlier (Carboniferous–Early Permian; Wang et al., 1987) than the high-pressure metamorphism (Late Triassic; Li et al., 1995; Kapp et al., 2003). However, the extensional exhumation of the Qiangtang metamorphic belt, which forms the basis of the mélange underthrusting model (Kapp et al., 2000, 2003) can also be well explained by the in situ suture model (Zhang, 2001), since such extensional exhumation of high- to ultrahigh-metamorphic rocks is common in orogens worldwide (e.g., Dewey, 1988). Nevertheless, the in situ suture zone and mélange underthrusting models have fundamental differences for the first-order crustal structure and accretionary history of the central Tibetan Plateau (Kapp et al., 2003). The origin of the Qiangtang metamorphic belt thus forms a key aspect for understanding the present development of the Tibetan Plateau and the evolution of the Tethys.

Theoretically, the correlative units within the Qiangtang metamorphic belt and the Jinsa suture zone should have closely similar geochemical fingerprints if the mélange underthrusting model is right. The purpose of this paper is to document and compare the geochemical characteristics of the two main rock types, metasiliciclastic rocks and metamafic igneous rocks, in these two tectonic entities in an attempt to evaluate their affinity and to constrain the origin of the Qiangtang metamorphic belt. Our geochemical results reveal that both metasiliciclastic rocks and metamafic igneous rocks within these two tectonic entities possess distinct geochemical signatures that most likely reflect their development in different tectonic settings.

## ANALYTICAL METHODS

A total of 74 fresh, representative samples were collected from two profiles in the Qiangtang metamorphic belt (32 samples) and the Jinsa suture zone (42 samples) (Figs. 1B and DR1[1]; Table DR1). The two profiles in the Qiangtang metamorphic belt are located in the areas that were mapped in detail by Kapp et al. (2000, 2003). The samples from these profiles include both metamorphic siliciclastic rocks and metamorphic mafic igneous rocks; however, the metamafic rocks are rare in our two profiles in the Jinsa suture zone, and their samples are thus limited (6 samples). All these siliciclastic rocks could be Triassic in age and could have formed in accretionary prism environments. Petrographic examination was carried out by both microscope and X-ray diffractometer (XRD). Fresh rock samples were then powdered to 200 mesh in an agate mill to avoid contamination. Fused-glass discs and pressed-powder discs were prepared for major-element and trace-element analysis (Ni, Co, Cu, Zn, V, Cr), respectively, by ARL9800$^+$ X-ray fluorescence at the Material Analysis Center of the Nanjing University. Accuracy is within 10% for trace elements and better than 5% for major elements. Loss on ignition (LOI) was determined at 980 °C for 90 min. Trace-element data, including rare earth elements (REEs), were obtained with standard inductively coupled plasma–mass spectrometer (ICP-MS) procedures at Finni-

*E-mail: kaijun@gig.ac.cn

[1]GSA Data Repository item 2006093, sample locations and geochemical analytical data, is available online at www.geosociety.org/pubs/ft2006.htm, or on request from editing@geosociety.org or Documents Secretary, GSA, P.O. Box 9140, Boulder, CO 80301, USA.

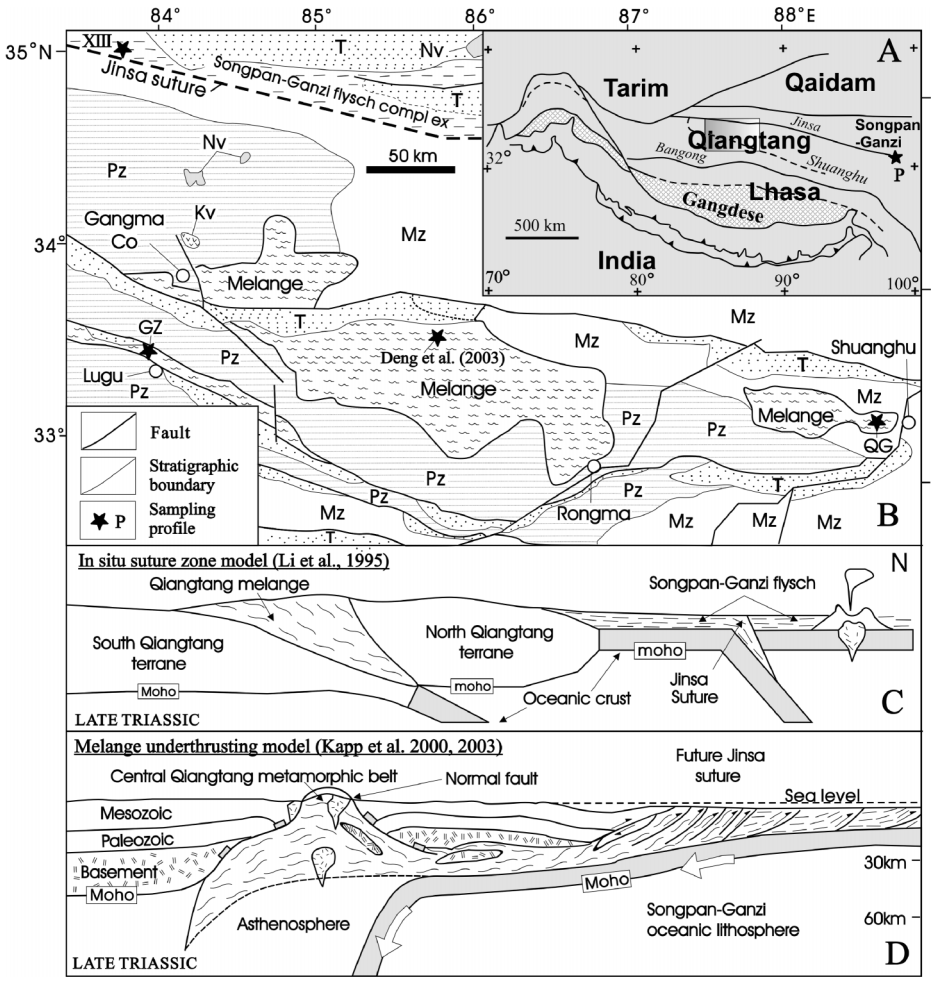


**Figure 1. A: Tectonic sketch map of Tibet, western China. B: Tectonic sketch map of the Qiangtang metamorphic belt. C: In situ suture zone model of the Qiangtang metamorphic belt (Li et al., 1995, 2002). D: Mélange underthrusting model (Kapp et al., 2000, 2003). B–D: simplified from Kapp et al. (2003). Kv—Cretaceous volcanic rocks; Mz—Mesozoic strata; Nv—Neogene volcanic rocks; Pz—Paleozoic strata; T—Tertiary nonmarine strata.**

gan MAT Element 2, at the State Key Laboratory of Mineral Deposit Research of Nanjing University, as described in detail by Zhang (2004). The reproducibility of measurements, based on measures of U.S. Geological Survey (USGS), Geological Survey of Japan (GSJ), and Institute of Geophysical and Geochemical Exploration (IGGE) standards, is better than 5% ($2\sigma$) for all the REEs, and the analytical error is generally less than 5% ($2\sigma$) for elements >10 ppm, and less than 8% for those <10 ppm. The geochemical data are presented in Table DR1.

## GEOCHEMISTRY

### Metasiliciclastic Rocks

The metasiliciclastic rocks from the two Qiangtang profiles (GZ and QG, Fig. 1B) occur as the matrix of the mélange and are mostly quartz schists with minor slates, in which relict sedimentary beds and arenaceous texture can be clearly observed. They display nearly identical petrologic and geochemical characteristics. These rocks are distinguished from the lesser deformed, sedimentary blocks of likely in situ origin within the metamorphic belt (Kapp et al., 2003) by intensive deformation and metamorphism. These rocks have a high $SiO_2$ (82.34 ± 5.16%) and moderate $Al_2O_3$ (7.40 ± 3.34%) and $K_2O$ (1.75 ± 0.75%) contents and low concentrations of $TiO_2$ (0.55 ± 0.16%), $Fe_2O_3$* (3.09 ± 1.07%), MgO (0.72 ± 0.40%), $Na_2O$ (0.53 ± 0.71%), CaO (1.04 ± 1.39%), as well as loss on ignition (LOI, 2.35 ± 1.23%). Although the absolute concentrations of REEs (182.76 ± 64.75 ppm) are variable, overall, the chondrite-normalized patterns of the siliciclastic rocks in the area are similar to the upper continental crust and North American Shale Composite (NASC; Gromet et al., 1984), with distinctive negative Eu anomalies (Eu/Eu*, 0.55 ± 0.10), light rare earth element (LREE) enrichment ($[La/Yb]_n$, 14.77 ± 3.35), and flat heavy rare earth element (HREE) distribution ($[Gd/Yb]_n$, 1.87 ± 0.43). These rocks also exhibit low ferromagnesian trace-element contents (Sc, 5.69 ± 2.96 ppm; Co, 6.91 ± 2.00 ppm; Cr, 54.39 ± 13.76 ppm; Ni, 13.76 ± 6.86 ppm).

The metasiliciclastic rocks from the two Jinsa profiles (P in Fig. 1A and XIII in Fig. 1B) also exhibit similar petrologic and geochemical characteristics. They are weakly metamorphosed slates, siltstones, and fine-grained feldspathic and lithic graywackes. The lithic grains in the sandstones include volcanic, siltstones, and sandstone fragments. In comparison with their Qiangtang counterparts, these Jinsa rocks have clearly low $SiO_2$ (65.51 ± 5.33%), $TiO_2$ (0.42 ± 0.07%), and $K_2O$ (1.45 ± 0.32%), but higher $Al_2O_3$ (8.67 ± 2.34%), $Fe_2O_3$* (3.43 ± 0.80%), MgO (2.19 ± 0.62%), $Na_2O$ (1.45 ± 0.83%), CaO (7.36 ± 4.05%), and LOI (9.24 ± 3.72%) contents. They also exhibit distinctly lower concentrations of REEs (151.07 ± 25.11 ppm), lesser LREE enrichment ($[La/Yb]_n$, 11.67 ± 1.64), flatter HREE distribution ($[Gd/Yb]_n$, 1.74 ± 0.15), and apparently higher Eu anomalies (Eu/Eu*, 0.62 ± 0.07). Relative to rocks in the Qiangtang metamorphic belt, these rocks display obviously higher ferromagnesian trace-element contents (Sc, 7.24 ± 1.58 ppm; Co, 9.00 ± 1.76 ppm; Cr, 56.2 ± 7.16 ppm; Ni, 21.08 ± 5.59 ppm).

### Metabasalts

Although the basalts from these two terrains are metamorphosed to greenschist facies, typical volcanic structures can still be observed, including vesicular and amygdaloidal structures. The basalts occur as variably deformed, meter-scale blocks enveloped in the matrix of metamorphosed siliciclastic rocks. The metabasalts and minor picrites from the Qiangtang metamorphic belt are characterized by (1) high $TiO_2$ (2.91 ± 0.84%) but low $Al_2O_3$ (9.27 ± 2.17%), (2) high REE concentrations (135.71 ± 57.94 ppm) and apparent LREE enrichment ($[La/Yb]_n$, 9.10 ± 4.15) but no Eu anomalies (Eu/Eu*, 0.99 ± 0.05) (Fig. 2A), (3) extremely high ferromagnesian trace-element contents (Sc, 29.10 ± 5.90 ppm; Co, 61.21 ± 15.35 ppm; Cr, 693 ± 422 ppm; Ni, 416 ± 266 ppm), (4) no Nb-Ta deletions related to Th and enrichment of other highly incompatible elements (Fig. 2B). Our geochemical results are nearly the same as those reported by Deng et al. (2002) from a more northern profile in the Qiangtang metamorphic belt (Fig. 1B).

However, in contrast to their Qiangtang counterparts, the metamafic rocks from Jinsa are characterized by (1) low to moderate $TiO_2$ (0.96 ± 0.29%) and moderate $Al_2O_3$ (17.94 ± 3.58%), (2) low REE concentrations (34.23 ± 13.50 ppm) and approximately flat REE patterns ($[La/Yb]_n$, 1.16 ± 0.24) (Fig. 2A), (3) moderate contents of ferromagnesian trace elements (Sc, 39.28 ± 8.70 ppm; Co, 39.10 ±

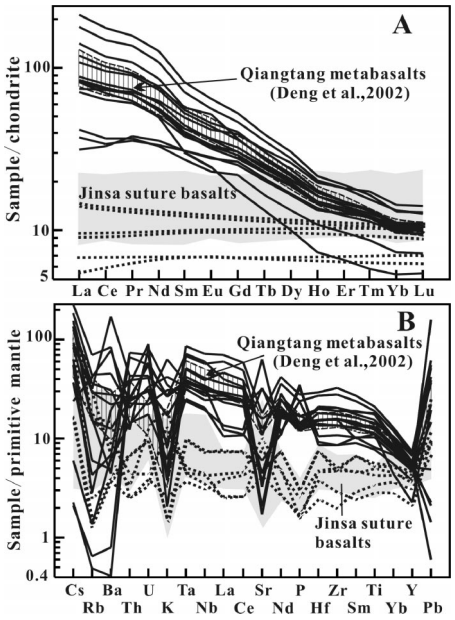


**Figure 2. Chondrite- (A) and primitive-mantle-normalized (B) spidergrams for metabasalts from the Qiangtang metamorphic belt (solid lines) and the Jinsa suture (dotted lines). Note the distinction between these two tectonic entities. The chondrite and primitive mantle values are from Anders and Grevesse (1989) and McDonough and Sun (1995), respectively. The metabasalts of the Jinsa suture are from Mo et al. (1993) and Xu and Castillo (2004).**

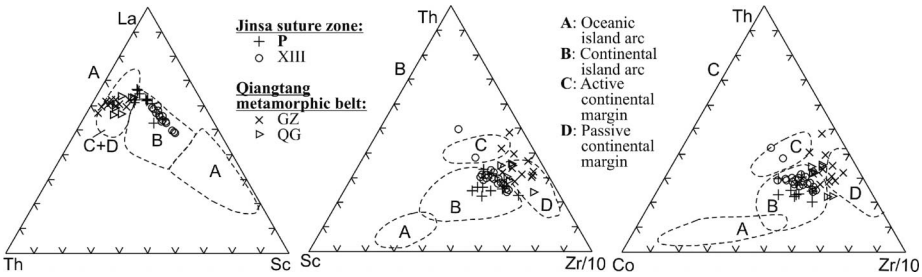


**Figure 3. La-Th-Sc (A), Th-Sc-Zr/10 (B), and Th-Co-Zr/10 (C) plots of the metamorphic siliciclastic rocks from the Qiangtang metamorphic belt and the Jinsa suture for tectonic discrimination. The dominant fields for various tectonic settings follow Bhatia and Crook (1986).**

9.34 ppm; Cr, 198 ± 196 ppm; Ni, 73.38 ± 59.82 ppm), (4) no Nb-Ta deletions related to Th (Fig. 2B). All the results are consistent with previous investigations along the Jinsa suture zone (e.g., Pearce and Deng, 1988; Mo et al., 1993; Xu and Castillo, 2004).

## DISCUSSION

### Distinctions Between the Qiangtang Metamorphic Belt and the Jinsa Suture Zone

Petrographical and geochemical observations indicate that metamorphosed siliciclastic rock samples collected from the Qiangtang metamorphic belt were derived from significantly more mature sources than those collected from the Jinsa suture zone. The apparently higher $SiO_2$ contents and $SiO_2/Al_2O_3$ ratios (14.28 ± 8.27), and lower $Na_2O$ and ferromagnesian contents and Eu anomalies of the Qiangtang samples, relative to their Jinsa counterparts ($SiO_2/Al_2O_3$, 7.93 ± 1.53), indicate that the former contain much more quartz and less plagioclase and have lower ferromagnesian contents than the latter, which is consistent with the petrographical studies. On conventional tectonic discriminatory plots using immobile elements, all the Qiangtang samples fall into the field for passive continental margins, but their Jinsa counterparts plot in the fields for continental island arcs and active continental margins (Fig. 3). Although depositional processes and metamorphism could influence the so-called immobile elements, the consistency of the conclusions about the provenance of the sediments from both major and trace elements suggests that they are reliable.

Mafic igneous samples analyzed contain 1.7%–12.9% $CO_2$, however, their altered nature hence inhibits the use of many of the standard major-element plots. For this reason, an evaluation of nonmobile elements, i.e., high field strength elements (HFSE) was carried out (Winchester and Floyd, 1976). The mafic rocks from the Qiangtang metamorphic belt and the Jinsa suture are geochemically distinct. For example, in the $P_2O_5$ versus $TiO_2$ diagram (Fig. 4A), the Qiangtang metabasalt samples fall into the oceanic-island or the within-plate basalt fields, whereas the Jinsa metamafic samples plot in the MORB field. The Qiangtang mafic rocks are highly enriched in LREEs, but those from Jinsa display flat REE chondrite-normalized patterns (Fig. 2A) (Mo et al., 1993; Xu and Castillo, 2004). The LREE enrichment of the Qiangtang rocks cannot be attributed to crustal contamination or fractionation due to the absence of Nb-Ta and Eu anomalies (Figs. 2A and 2B) as well as high positive $\varepsilon_{Nd}$ values relative to the mantle (+5.5 to +11.3, Li et al., 2002). The concentrations of highly incompatible elements in the Qiangtang rocks are typical of oceanic alkali basalts (Engel et al., 1965) and far exceed those of either N- or P-MORB (Sun et al., 1979), whereas the Jinsa samples are characteristic of tholeiitic basalts (Pearce and Deng, 1988; Mo et al., 1993; Xu and Castillo, 2004). On a Zr/Y versus Zr diagram (Fig. 4B), the samples from Jinsa and Qiangtang similarly form two distinct suites. The former plot within the MORB field, while the latter fall in the within-plate field. A similar bimodal distribution is exhibited on the V-Ti and Nb-Zr-

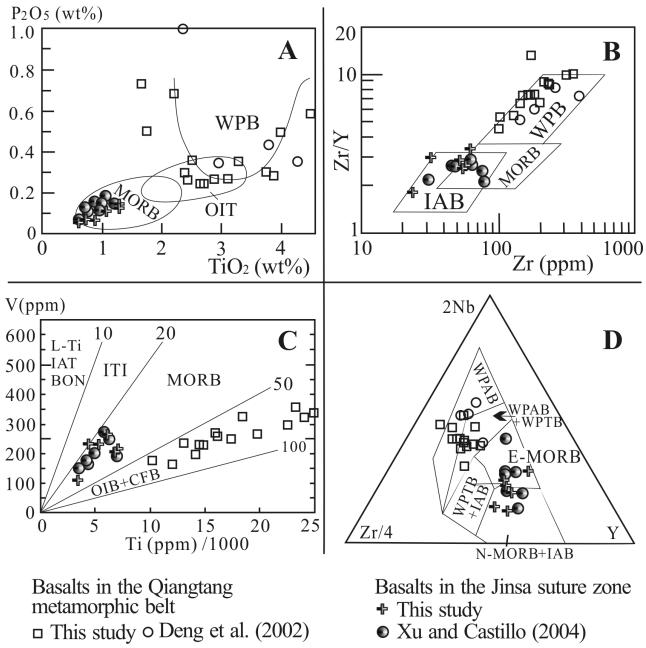


**Figure 4. Tectonomagmatic discrimination diagrams for the metabasalts from the Qiangtang metamorphic belt and the Jinsa suture. A: $P_2O_5$ versus $TiO_2$ diagram of Bass et al. (1973). B: Zr/Y versus Zr of Pearce and Norry (1979). C: V versus Ti diagram of Shervais (1982). D: Nb-Zr-Y diagram of Meschede (1986). Note that the Jinsa basalts could have been produced in a mid-ocean ridge environment, while the Qiangtang basalts formed in a within-plate oceanic-island setting. BON—boninite; CFB—continental flood basalt; IAT—island-arc tholeiite; IAB—island-arc basalt; MORB—mid-oceanic-ridge basalt; E-MORB—basalts from plume-influenced regions; N-MORB—normal mid-oceanic-ridge basalt; OIB—oceanic-island basalt; OIT—oceanic-island tholeiite; WPB—within-plate basalt; WPAB—within-plate alkali basalt; WPTB—within-plate tholeiitic basalt; L-Ti—low Ti.**

Y plots (Figs. 4C and 4D). On both plots, the Jinsa basalts again fall in the MORB field, whereas the Qiangtang samples fall in the within-plate basalt field or the alkaline field, nearly the same as in the Zr/Y versus Zr plot. Therefore, along with the $P_2O_5$ versus $TiO_2$ diagram (Fig. 4A), we conclude that the Jinsa basalts were most likely produced in a mid-ocean ridge environment, while the Qiangtang basalts formed in a within-plate oceanic-island setting.

## Origin of the Qiangtang Metamorphic Belt

The geochemical distinction of metasiliciclastic rocks and metabasalts in the Qiangtang metamorphic belt from those in the Jinsa suture zone suggests that there is no affinity between these two tectonic entities and that the Jinsa suture zone is not the source of the Qiangtang metamorphic belt. The alkali basalts with oceanic-island basalt (OIB) features in the Qiangtang metamorphic belt (Figs. 4A–4D) are most likely derived from a plume source and are possibly related to the Permian mantle plume activities across the paleo-Tethys (e.g., Chung et al., 1998). They could have formed a seamount sequence in which an internal core of massive basalt is overlain by volcanic-siliciclastic flank debris flow facies. Bedded cherts (e.g., Li et al., 1997) and marbles (e.g., Li et al., 1995; Kapp et al., 2003) within the Qiangtang metamorphic belt are regarded as ancient pelagic sediments with shallow-water capping carbonates that developed on basaltic seamounts. Such seamounts can subduct at a trench partially or in their entirety. More recent mapping shows that the metamorphic belt is well exposed in the Qiangtang terrain, approximately along the Shuanghu suture zone delineated in Figure 1A (GSC and CIGMR, 2004). Moreover, the detrital zircon age spectra of Qiangtang metasandstones (Kapp et al., 2003) are closely similar to those of the Himalaya (e.g., Myrow et al., 2003), indicating that a northern provenance of Qiangtang metasandstones (Kapp et al., 2003) is unnecessary. We thus believe that the Qiangtang metamorphic belt represents a distinct and unrelated paleo-Tethyan suture zone that separates northern and southern Qiangtang terranes. The southward subduction of the Songpan-Ganzi terrain detected by the metasedimentary xenoliths in Cenozoic volcanic rocks (e.g., Hacker et al., 2000) could be a much later event, possibly triggered by the Indian collision.


## ACKNOWLEDGMENTS

This research was supported by the Chinese Academy of Science Hundred Talents Project and the Natural Science Foundation of China (grant 40572137). We are grateful to T.P. Zhao and L.F. Zhong for help in fieldwork, to J.F. Gao, Y. Liu, and M.Q. Zhang for analytical support, to Roger D. Brewer for assistance in editing the original manuscript, and to Jonathan Aitchison, Tina M. Niemi, and Lothar Ratschbacher for helpful reviews.


## REFERENCES CITED


Anders, E., and Grevesse, N., 1989, Abundances of the elements: Meteoritic and solar: Geochimica et Cosmochimica Acta, v. 53, p. 197–214, doi: 10.1016/0016-7037(89)90286-X.

Bao, P.S., Xiao, X.C., Wang, J., Li, C., and Hu, K., 1999, The blueschist belt in the Shuanghu region, central-northern Tibet, and its tectonic implications: Acta Geologica Sinica, v. 73, p. 302–314.

Bass, M.N., Moberly, R., and Rhodes, J.M., 1973, Volcanic rocks cored in the central Pacific, Leg 17: Initial Reports of the Deep Sea Drilling Project, v. 17, p. 429–503.

Bhatia, M.R., and Crook, K.A.W., 1986, Trace element characteristics of greywackes and tectonic setting discrimination of siliciclastic basin: Contributions to Mineralogy and Petrology, v. 92, p. 181–193, doi: 10.1007/BF00375292.

Chung, S.L., Jahn, B.M., Wu, G.Y., Lo, C.H., and Cong, B.L., 1998, The Emeishan flood basalt in SW China: A mantle plume initiation model and its connection with continental breakup and mass extinction at the Permian-Triassic boundary: Geodynamics Series, v. 27, p. 47–58.

Deng, W.M., Yin, J., and Guo, Z., 1996, Basic-ultrabasic and volcanic rocks in Chagbu-Shuanghu area of northern Xizang (Tibet), China: Science in China: Series D, v. 39, p. 359–368.

Deng, X.G., Ding, L., Liu, X.H., Yin, A., Kapp, P., Murphy, M.A., and Manning, C.E., 2002, Geochemical characteristics of the blueschists and its tectonic significance in the central Qiangtang area, Tibet: Acta Petrologica Sinica, v. 18, p. 517–525.

Dewey, J.F., 1988, Extensional collapse of orogens: Tectonics, v. 9, p. 1123–1139.

Engel, A.E., Engel, S.E., and Havens, R.V., 1965, Chemical characteristics of oceanic basalts and the upper mantle: Geological Society of America Bulletin, v. 76, p. 719–734.

Gromet, L.P., Dymek, R.F., Haskin, L.A., and Korotev, R.L., 1984, The North American shale composite: Its compilation, major and trace element characteristics: Geochimica et Cosmochimica Acta, v. 48, p. 2469–2482, doi: 10.1016/0016-7037(84)90298-9.

GSC (Geological Survey of China), and CIGMR (Chengdu Institute of Geology and Mineral Resources), 2004, Geological map of Tibet (China) and adjacent areas (1:1,500,000) with an explanation: Chengdu, Chengdu Cartographic Press, 133 p.

Hacker, B., Gnos, E., Ratschbacher, L., Grove, M., McWilliams, M., Sobolev, S., Jiang, W., and Wu, Z., 2000, Hot and dry deep crustal xenoliths from Tibet: Science, v. 287, p. 2463–2466, doi: 10.1126/science.287.5462.2463.

Kapp, P., Yin, A., Manning, C.E., Murphy, M., Harrison, T.M., Spurlin, M., Ding, L., Deng, X.G., and Wu, C.M., 2000, Blueschist-bearing metamorphic core complexes in the Qiangtang block reveal deep crustal structure of northern Tibet: Geology, v. 28, p. 19–22, doi: 10.1130/0091-7613(2000)028<0019:BBMCCI>2.3.CO;2.

Kapp, P., Yin, A., Manning, C.E., Harrison, T.M., and Taylor, M.H., 2003, Tectonic evolution of the early Mesozoic blueschist-bearing metamorphic belt, central Tibet: Tectonics, v. 24, 1043, doi: 1029/2002TC001383.

Li, C., Cheng, L.R., Hu, K., Yang, Z.R., and Hong, Y.R., 1995, Study on the paleo-Tethys suture zone of Longmu Co-Shuanghu, Tibet: Beijing, Geological Publishing House, 131 p.

Li, C., Li, Y.T., Lin, Y.X., Wang, T.W., Yang, D.M., and He, Z.H., 2002, Sm-Nd dating of the protoliths of blueschist in the Shuanghu area, Tibet: Geology in China, v. 29, p. 355–360.

Li, Y.J., Wu, H.R., Li, H.S., and Sun, D.L., 1997, Discovery of radiolarians in the Amugang and Chasang Groups and Lugu Formation in northern Tibet and discussion on some problems: Geological Review, v. 43, p. 250–257.

McDonough, W.F., and Sun, S.S., 1995, The composition of the Earth: Chemical Geology, v. 120, p. 223–253, doi: 10.1016/0009-2541(94)00140-4.

Meschede, M., 1986, A method of discriminating between different types of mid-ocean ridge basalts and continental tholeiites with the Nb-Zr-Y diagram: Chemical Geology, v. 56, p. 207–218, doi: 10.1016/0009-2541(86)90004-5.

Mo, X.X., Lu, F.X., and Shen, S.Y., 1993, Volcanism and mineralization of the three-river Tethys (Tibet, western China): Beijing, Geological Publishing House, 234 p.

Myrow, P.M., Hughes, N.C., Paulsen, T.S., Williams, I.S., Parcha, S.K., Thompson, K.R., Bowring, S.A., Peng, S.C., and Ahluwalia, A.D., 2003, Integrated tectonostratigraphic analysis of the Himalaya and implications to its tectonic reconstruction: Earth and Planetary Science Letters, v. 212, p. 433–441, doi: 10.1016/S0012-821X(03)00280-2.

Pearce, J.A., and Deng, W.M., 1988, The ophiolites of the Tibetan Geotraverses, Lhasa to Golmud (1985) and Lhasa to Kathmandu (1986): Royal Society of London Philosophical Transactions, ser. A, v. 327, p. 215–238.

Pearce, J.A., and Norry, M.J., 1979, Petrogenetic implications of Ti, Zr, Y, and Nb variations in volcanic rocks: Contributions to Mineralogy and Petrology, v. 69, p. 33–47, doi: 10.1007/BF00375192.

Shervais, J.W., 1982, Ti-V plots and the petrogenesis of modern and ophiolitic lavas: Earth and Planetary Science Letters, v. 59, p. 101–118, doi: 10.1016/0012-821X(82)90120-0.

Sun, S.S., Nesbitt, R.W., and Sharaskin, A.Y., 1979, Geochemical characteristics of mid-ocean basalts: Earth and Planetary Science Letters, v. 44, p. 119–138, doi: 10.1016/0012-821X(79)90013-X.

Wang, C.S., Hu, C.Z., and Wu, R.Z., 1987, Discovery and geologic significance of the Casang-Cabu rift in northern Xizang: Bulletin of Chengdu College of Geology, v. 14, p. 33–46.

Winchester, J.A., and Floyd, P.A., 1976, Geochemical magma type discrimination: Application to altered and metamorphosed basic igneous rocks: Earth and Planetary Science Letters, v. 28, p. 459–469, doi: 10.1016/0012-821X(76)90207-7.

Xia, B.D., Li, C., and Ye, H.F., 2001, Blueschist-bearing metamorphic core complexes in the Qiangtang terrain reveal deep crustal structure of northern Tibet: Comment: Geology, v. 29, p. 663, doi: 10.1130/0091-7613(2001)029<0663:BBMCCI>2.0.CO;2.

Xu, J.F., and Castillo, P.R., 2004, Geochemical and Nd-Pb isotopic characteristics of the Tethyan asthenosphere: Implications for the origin of the Indian Ocean mantle domain: Tectonophysics, v. 393, p. 9–27, doi: 10.1016/j.tecto.2004.07.028.

Yin, A., and Harrison, T.M., 2000, Geologic evolution of the Himalayan-Tibetan orogen: Annual Review of Earth and Planetary Sciences, v. 28, p. 211–280, doi: 10.1146/annurev.earth.28.1.211.

Zhang, K.J., 2001, Blueschist-bearing metamorphic core complexes in the Qiangtang terrain reveal deep crustal structure of northern Tibet: Comment: Geology, v. 29, p. 90, doi: 10.1130/0091-7613(2001)029<0090:BBMCCI>2.0.CO;2.

Zhang, K.J., 2004, Secular geochemical variations of the Lower Cretaceous siliciclastic rocks from central Tibet (China) indicate a tectonic transition from continental collision to back-arc rifting: Earth and Planetary Science Letters, v. 229, p. 73–89, doi: 10.1016/j.epsl.2004.10.030.



Manuscript received 6 November 2005
Revised manuscript received 23 January 2006
Manuscript accepted 3 February 2006

Printed in USA